Phytochemistry 71 (2010) 262–270

Contents lists available at ScienceDirect

Phytochemistry

journal homepage: www.elsevier.com/locate/phytochem

Bioactive microbial metabolites from glycyrrhetinic acid

Galal T. Maatooq [a], Amani M. Marzouk [a,*], Alexander I. Gray [b], John P. Rosazza [c]

[a] Department of Pharmacognosy, Faculty of Pharmacy, Mansoura University, Mansoura 35516, Egypt
[b] Department of Pharmaceutical Sciences, Strathclyde Institute for Biomedical Sciences, University of Strathclyde, Glasgow G4 0NR, Scotland, UK
[c] Division of Medicinal and Natural Products Chemistry, College of Pharmacy and Centre for Biocatalysis and Bioprocessing, University of Iowa, IA 52242, USA

ARTICLE INFO

Article history:
Received 21 April 2009
Received in revised form 14 September 2009
Available online 14 October 2009

Keywords:
18β-Glycyrrhetinic acid
Microbial transformation
Hepatoprotection
Lipid peroxidation
Nitric oxide

ABSTRACT

Biotransformation of 18β-glycyrrhetinic acid, using *Absidia pseudocylinderospora* ATCC 24169, *Gliocladium viride* ATCC 10097 and *Cunninghamella echinulata* ATCC 8688a afforded seven metabolites, which were identified by different spectroscopic techniques (^{1}H, ^{13}C NMR, DEPT, ^{1}H-^{1}H COSY, HMBC and HMQC). Three of these metabolites, *viz*. 15α-hydroxy-18α-glycyrrhetinic acid, 13β-hydroxy-7α,27-oxy-12-dihydro-18β-glycyrrhetinic acid and 1α-hydroxy-18β-glycyrrhetinic acid are new. The ^{13}C NMR data and full assignment for the known metabolite 7β, 15α-dihydroxy-18β-glycyrrhetinic acid are described here for the first time. The major metabolites were evaluated for their hepatoprotective activity using different *in vitro* and *in vivo* models. These included protection against $FeCl_3$/ascorbic acid-induced lipid peroxidation of normal mice liver homogenate, induction of nitric oxide (NO) production in rat macrophages and *in vivo* hepatoprotection against CCl_4-induced hepatotoxicity in albino mice.

1. Introduction

18β-Glycyrrhetinic acid (**1**) is the active form of glycyrrhizin which is the major pentacyclic triterpene in licorice (*Glycyrrhiza glabra* L.). It has been shown to possess several pharmacological activities, such as antiulcerative, anti-inflammatory, immunomodulating (Chung et al., 2001) and antitumour activities (Ryu et al., 1994; Luo et al., 2004). In addition, direct and indirect antiviral activity, interferon-inducibility and antihepatitis effects have been attributed to glycyrrhetinic acid (Barran et al., 1974; Mahato et al., 1992). It is extensively used in Japan and has been examined in Europe in patients with acute and chronic hepatitis to reduce the progression of liver disease to hepatocellular carcinoma (Arase et al., 1997; Van Rossum et al., 1998). A recent report showed that glycyrrhetinic acid also reverses the multidrug resistance to cancer chemotherapeutic agents and can be considered as a promising lead compound for the design of more efficacious and less toxic chemosensitizing agents to enhance the efficacy of cancer chemotherapy (Nabekura et al., 2008). Glycyrrhetinic acid was previously subjected to several studies to obtain new useful derivatives *via* semisynthesis (Ignatov et al., 2003) or microbial transformation (Canonica et al., 1967; Yamada et al., 1994; Yoshida et al., 2001a, b,c; Xin et al., 2006). In this work, we describe the isolation and structural elucidation of seven microbial metabolites of glycyrrhetinic acid (**2**–**8**) (Fig. 1) produced by *Absidia pseudocylinderospora* ATCC 24169, *Cunninghamella echinulata* ATCC 8688a and *Gliocladium viride* ATCC 10097. Three of these metabolites are new (**6**–**8**). The major metabolites (**2**) and (**7**) were evaluated for their hepatoprotective activity against the parent compound using different *in vitro* and *in vivo* models.

2. Results and discussion

In many cases, structural modification of natural bioactive compounds leads to interesting results. New compounds turn out to be more effective and exhibit a wider spectrum of activities and/or less toxicity. Microbial transformation provides many advantages over chemical derivatization. These include high catalytic activity and high regio-and stereo specificity (Kieslich, 1976). In this work we tried to get new derivatives through microbial transformation of glycyrrhetinic acid which is an interesting lead compound of versatile activities. Biotransformation of glycyrrhetinic acid (**1**) with *A. pseudocylinderospora* ATCC 24169, *C. echinulata* ATCC 8688a and *G. viride* ATCC 10097 afforded seven metabolites (**2**–**8**). We also tested the major metabolites (**2** and **7**) for their hepatoprotective activity, in both *in vivo* and *in vitro* systems. Scaling up the reaction with *A. pseudocylinderospora* ATCC 24169 afforded **2** as the major metabolite. A dioxygenated derivative of glycyrrhetinic acid was suggested based on a 32 mass unit increase over that of **1**, where metabolite **2** gave a molecular ion peak in HRESI spectrum (negative ion mode) at *m/z* 502.3251 $[M]^-$, (calc. 502.3294) indicating a molecular formula of $C_{30}H_{46}O_6$. Hydroxylation was suggested by the appearance of two new methine carbinol protons at δ 4.53 (1 H, *dd*, *J* = 4.9, 11.2 Hz) and 4.71 (1 H, *dd*, *J* = 5.2, 11.7 Hz) in the ^{1}H NMR spectrum (Table 1), which were correlated by

* Correspondence author. Fax: +20 50 2247496.
E-mail address: amarzouk2003@yahoo.co.uk (A.M. Marzouk).

0031-9422/$ - see front matter © 2009 Elsevier Ltd. All rights reserved.
doi:10.1016/j.phytochem.2009.09.014

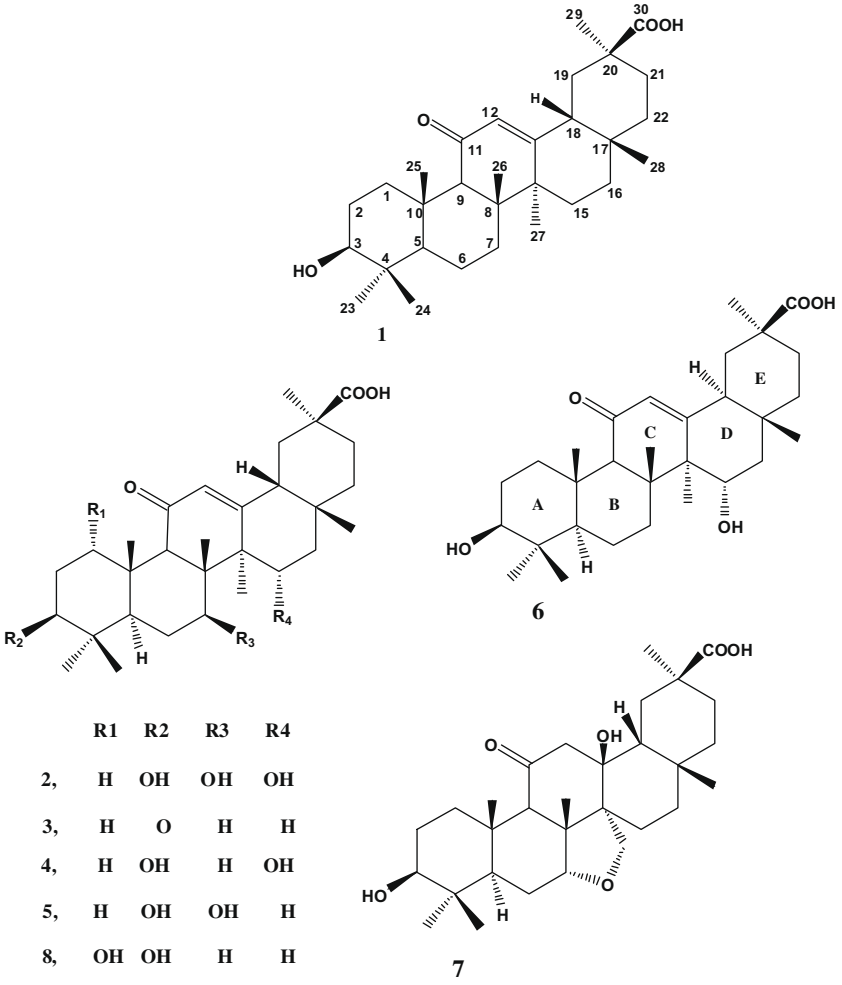

Fig. 1. Structure of 18β-glycyrrhetinic acid (**1**) and its metabolites.

HMQC to carbon resonances at δ 72.2 and 67.2, respectively. The assignment of these carbon resonances to positions 7 and 15 was confirmed by observation of β and γ effects on the chemical shifts of the carbon atoms in their vicinities, as well as by HMBC experiment. β-Effect was evident as deshielding at positions 6 and 16 (δ 28.5 and 36.7) which showed downfield shifts by 11.0 and 10.2 ppm, respectively, compared to glycyrrhetinic acid (Table 2). γ-Effect was evidenced by shielding of positions 5 and 26 (δ 52.6 and 13.9) by 2.3 and 4.8 ppm, respectively. Positions which are mutually affected by β and γ effects *viz*., positions 8 and 14 (δ 52.4 and 51.1) suffered a net result of deshielding by 9.2 and 5.6 ppm, respectively. The HMBC spectrum (Fig. 2) showed cross peaks between H-7 (δ 4.53, *dd*, *J* = 4.9, 11.2 Hz) and each of C-5, 6, 8 and 14 (δ 52.6, 28.5, 52.4 and, 51.1), while H-15 (δ 4.71, *dd*, *J* = 5.2, 11.7 Hz) showed cross peaks with each of C-8, 14, 16, 17 and 27 (δ 52.4, 51.1, 36.7, 32.9 and 19.4). The orientations of the hydroxyl groups at C-7 and C-15 were confirmed to be β and α, respectively, through NOESY experiment (Fig. 3). NOE effects were observed between H-7 and each of C-27 methyl protons signal (δ 1.76, s) and H-6 *eq* (δ 2.19, *br dd*), while H-15 interacted with each of the methyl protons singlets of C-26 and C-28 (δ 1.48 and 0.93), respectively. These data confirmed the structure of **2** as 7β,15α-dihydroxy-18β-glycyrrhetinic acid. This compound was identified before by ^{1}H NMR as one of the microbial metabolites of glycyrrhetinic acid transformed with *Trichothecium roseum* ATCC 8685 (Canonica et al., 1967). The ^{13}C NMR data and full assignment are presented here for the first time.

Scaling up the reaction with *G. viride* ATCC 10097 afforded metabolite **3**. HRESIMS (negative ion mode) showed a molecular ion peak at *m/z* 468.3210 $[M]^-$ indicating a molecular formula of $C_{30}H_{44}O_4$. (calc. 468.3239). Comparison of the NMR data of **3** to that of **1** (Tables 1 and 2) revealed that metabolite, **3,** is the 3-oxo derivative of glycyrrhetinic acid. This was strongly suggested by the disappearance of the methine proton signal at position 3 of glycyrrhetinic acid (δ 3.25, *dd*, *J* = 5.7, 10.2 Hz) and the corresponding carbon at δ 78.9, in addition to the appearance of the new carbonyl resonance at δ 217.3. This assignment was confirmed by observing downfield shifts by 7.0 and 4.8 ppm of carbon atoms at positions 2 and 4 (δ 34.2 and 43.9), respectively. This compound has been identified before as a microbial metabolite of glycyrrhetinic acid by a number of *Aspergillus* species including *Aspergillus niger*, *Aspergillus oryzae*, *Aspergillus sojae* and *Aspergillus tamarii* (Yamada et al., 1994).

C. echinulata ATCC 8688a transformed glycyrrhetinic acid into five metabolites (**4–8**). ESIMS spectrum of **4** (negative ion mode) gave a molecular ion peak at *m/z* 486 $[M]^-$, calculated for the molecular formula $C_{30}H_{46}O_5$ and suggesting a monohydroxylated derivative. NMR data of **4** (Tables 1 and 2) led to its identification as 15α-hydroxy-18β-glycyrrhetinic acid, reported before as a biotransformation product of glycyrrhetinic acid with *Mucor polymorphosporus* (Xin et al., 2006) and *T. roseum* ATCC 8685 (Canonica et al., 1967).

Metabolite **5** gave a molecular ion peak in ESIMS (Negative ion mode) at *m/z* 486 $[M]^-$ calculated for the molecular formula

Table 1
^{1}H NMR data of glycyrrhetinic acid (**1**) and its metabolites **2–8**.[a]

H	**1**[b]	**2**[b]	**3**[c]	**4**[d]	**5**[d]	**6**[d]	**7**[d]	**8**[e]
1	0.95, *m* 2.79, *dt* (3.5, 13.5)	1.26, *m*, ax 3.25, *dt* (3.2, 10.2) eq	1.40, *m* 2.96, *m*	0.98, *m* 2.75, *dt* (3.5, 13.4)	0.95, *dd* (3.0, 13.3) 2.72, *dt* (3.4, 13.4)	1.01, *m* 2.58, *dt* (3.2, 13.2)	1.62, *m* 2.54, *dt* (3.5, 13.4)	4.38, m 4.41, *d* (4.5, OH ax)
2	1.42, *m* 1.58, *m*	1.92, *m*, ax 2.02, *m*, eq	2.36, *m* 2.64, *m*	1.53, *m* 1.67, *m*	1.50, *m* 1.66, *m*	1.51, *m* 1.69, *m*	1.50, *m* 1.63, *m*	1.50, *m* 1.76, *m*
3	3.25, *dd* (5.7, 10.2)	3.55, *dd* (4.4, 11.6)		3.16, *dd* (4.5, 11.7)	3.17, *dd* (4.6, 11.6)	3.17, *dd* (4.5,11.6)	3.15, *dd* (4.4,11.7)	3.44 *ddd* (4.9, 5.7, 11.5) 4.10, *d* (5.7, OH eq)
5	0.71, *m*	1.30, *m*	1.30, *dd* (3.4,11.2)	0.79, *m*	0.86, *m*	0.77, *m*	1.29, *m*	0.87, m
6	1.33, *m* 1.58, *m*	1.97, *m*, ax 2.19, *br dd*, eq	1.54, *m* 1.58, *m*	1.49, *m* 1.60, *m*	1.54, *m* 1.73, *m*	1.43, *m* 1.55, *m*	1.42, *m* 1.85, *m*	1.50, *m* 1.74, *m*
7	1.78, *m* 1.97, *m*	4.53 *dd* (4.9, 11.2)	1.46, *dt* (3.2, 15.5) 1.69, *m*	1.78, *dt* (3.2, 15.5) 1.98, *m*	4.08, *dd* (5.0, 11.0)	1.83, *m* 2.07, *m*	3.84*dd* (5.8, 11.4)	1.57, *m* 1.87, *m*
9	2.36, *s*	2.65, *s*	2.45, *s*	2.41, *s*	2.37, *s*	2.32, *s*	2.24, *s*	3.25, *s*
12	5.71, *br s*	6.20, *brs*	5.53, *s*	5.59, *brs*	5.57, *brs*	5.48, *d* (1.8)	2.96, *d* (15.7) 2.09, *d* (15.7)	5.37, *brs*
15	1.66, *m* 2.03, *m*	4.71, *dd* (5.2, 11.7)	1.21, *m* 1.85, *m*	4.27, *dd* (5.5, 11.3)	1.65, *m* 2.16, *m*	4.29, *dd* (5.2, 11.8)	1.39, *m* 2.12, *m*	1.14, *m* 1.24, *m*
16	2.01, *m* 1.25, *m*	1.60, *dd* (5.2, 13) 2.48, *dd* (11.7, 13)	1.12, *m* 2.04, *m*	1.26, *dd* (5.4, 13. 3) 2.14, *m*	1.12, *m* 2.15, *m*	1.49, *m* 1.65, *dd* (5.2, 13.8)	1.42, *m* 1.64, *m*	1.67, *m* 1.73, *m*
18	2.16, *m*	2.66, *m*	2.22, *m*	2.19, *dd* (4.2, 15.5)	2.21, *m*	2.29, *d* *t*(2.5, 11.7)	2.42, *ddd* (3.8, 3.8, 14.5)	2.05, *m*
19	1.66, *m* 1.83, *m*	1.93, *m* 2.27, *m*	1.61, *m* 1.93, *m*	1.78, *dd* (3.2, 15.5) 1.91, *m*	1.80, *dd* (3.2, 13.3) 1.87, *m*	1.37, *m* 2.03, *m*	1.61, *m* 1.82, *m*	1.15, *m* 1.66, *m*
21	1.40, *m* 1.91, *m*	1.51, *m*, eq 2.29, *m*, ax	1.32, *m* 2.01, *m*	1.41, *m* 1.96, *m*	1.42, *m* 1.95, *m*	1.42, *m* 2.05, *m*	1.83, *m* 1.87, *m*	1.49, *m* 2.09, *m*
22	1.35, *m* 1.39, *m*	1.52, *m*, ax 1.72, *m*, eq	1.39, *m* 1.43, *m*	1.35, *m* 1.41, *m*	1.38, *m* 1.42, *m*	1.18, *m* 2.03, *m*	1.23, *m* 1.99 *ddd* (3.5, 3.5,14.2)	0.85, *m* 0.99, *m*
23	1.00, *s*	1.32, *s*	1.07, *s*	1.00, *s*	1.00, *s*	0.99, *s*	0.98, *s*	0.89, *s*
24	0.81, *s*	1.22, *s*	1.05, *s*	0.79, *s*	0.80, *s*	0.80, *s*	0.77, *s*	0.66, *s*
25	1.13, *s*	1.44, *s*	1.26, *s*	1.13, *s*	1.10, *s*	1.23, *s*	1.19, *s*	1.00, *s*
26	1.14, *s*	1.39, *s*	1.17, *s*	1.19, *s*	1.14, *s*	1.19, *s*	1.38, *s*	1.03, *s*
27	1.38, *s*	1.76, *s*	1.38, *s*	1.44, *s*	1.50, *s*	1.30, *s*	3.71, *d* (8.6) 4.27, *dd* (8.6,2.2)	1.32, *s*
28	0.84, *s*	0.93, *s*	0.84, *s*	0.86, *s*	0.84, *s*	0.78, *s*	1.02, *s*	0.75, *s*
29	1.21, *s*	1.38, *s*	1.21, *s*	1.20, *s*	1.19, *s*	1.26, *s*	1.15, *s*	1.08, *s*

[a] Spectra run at 600 MHz, δ in ppm and J values (Hz) in parentheses.
[b] Measured in pyridine-d_5 relative to TMS at 500 MHz.
[c] Measured in $CDCl_3$ relative to TMS.
[d] Measured in acetone-d_6 relative to TMS.
[e] Measured in DMSO-d_6 relative to TMS.

$C_{30}H_{46}O_5$ and suggesting another monohydroxylated derivative of the substrate. Comparing the NMR data of **5** (Tables 1 and 2) to literature values, It was identified as 7β-Hydroxy-18β-glycyrrhetinic acid. This metabolite was obtained before as glycyrrhetinic acid metabolite by *M. polymorphosporus* (Xin et al., 2006).

NMR data of metabolite **6** indicated that it is a monohydroxylated derivative of glycyrrhetinic acid. An oxygenated carbon resonance at δ 67.2 which was correlated by HMQC experiment to a proton signal at δ 4.29 (*dd*, J = 5.2, 11.8 Hz) was assigned to position 15. Hydroxylation at this position was confirmed by HMBC experiment (Fig. 2). Cross peaks were observed between H-15 (δ 4.29, *dd*, J = 5.2, 11.8 Hz) and each of C-8, 14, 16, 17 and 27 (δ 51.4, 45.8, 49.0, 34.7 and 14.2, respectively); between C-15 (δ 67.2) and each of the protons of the methyl group at position 27 (δ 1.30, s) and both protons at H-16 (δ 1.49, m and 1.65, *dd*, J = 5.2, 13.8 Hz). The chemical shift of C-15 inferred α-hydroxyl group at this position. Comparison of the ^{13}C NMR data of **6** with that of **4** (Table 2) revealed that the chemical shifts of carbon atoms in rings A and B were almost identical. Significant differences appeared in chemical shifts of carbon atoms in the other rings as follows: in ring C, C-12 and 13 (δ 125.5 and 165.5) exhibited shielding by 3.8 and 4.9 ppm, respectively. In ring D, C-16 (δ 49.0) exhibited deshielding by 11.0 ppm compared to the same carbon in **4** (carbon resonance at δ 38.0), while C-18 (δ 43.4) appeared at 6.4 ppm higher field than the corresponding carbon in **4** (δ 49.8). C-28 methyl, similarly, showed shielding by 12.1 ppm. These effects could be ascribed to a new γ-gauche interaction between C-28 methyl and the axial protons at positions 19 and 21. Other positions were confirmed by HMBC (Fig. 2). Comparing these shift values with data published for different oleanane-type derivatives, they were found comparable to those of 18α-derivatives of glycyrrhetinic acid (Mahato and Kundu, 1994). Therefore, metabolite **6** was identified as 15α-hydroxy-18α-glycyrrhetinic acid, which is a new natural product. The inversion of the stereo chemistry at C-18 of glycyrrhetinic acid is described before to proceed from the 18β-epimer *via* the formation of 11,13(18)-dien-11-ol as intermediate product after treatment with HCl/MeOH (Ignatov et al., 2003). *C. echinulata* is one of the microorganisms reported to bring about stereoinversion. Microbial stereoinversion is thought to proceed *via* an oxidation–reduction sequence (SimeÓ et al., 2007). The inversion of

Table 2
^{13}C NMR data of glycyrrhetinic acid (**1**) and its metabolites (**2–8**).[a]

C	1[b]	2[c]	3[b]	4[e]	5[e]	6[e]	7[e]	8[d]
1	39.1	40.1	39.7	39.9	39.6	39.8	40.6	70.6
2	27.2	28.7	34.2	28.0	28.1	28.2	27.9	33.9
3	78.9	78.3	217.3	78.3	78.3	78.4	78.2	70.6
4	39.1	40.1	43.9	39.8	39.5	39.7	39.4	38.7
5	54.9	52.6	55.4	55.4	52.3	55.6	51.0	46.3
6	17.5	28.5	18.8	18.5	29.6	18.7	31.8	16.9
7	32.8	72.2	32.1	36.6	72.5	37.9	69.0	31.8
8	43.2	52.4	47.8	49.6	51.2	51.4	58.4	44.4
9	61.8	63.2	61.0	62.5	62.8	61.6	64.2	52.5
10	37.1	38.4	36.7	38.1	38.0	37.7	38.3	40.8
11	200.5	199.5	199.7	199.8	199.3	199.7	208.5	199.7
12	128.5	129.8	128.4	129.3	128.9	125.5	54.3	127.5
13	169.5	170.9	170.0	170.4	170.0	165.5	87.7	169.0
14	45.5	51.1	45.3	47.4	45.5	45.8	47.9	43.2
15	26.4	67.2	26.4	67.4	30.7	67.2	29.6	26.0
16	26.5	36.7	26.6	38.0	27.4	49.0	27.9	25.8
17	31.9	32.9	31.9	33.0	32.6	34.7	32.7	31.5
18	48.2	50.5	48.3	49.8	50.0	43.3	45.6	47.9
19	41.0	42.1	41.5	41.6	42.1	34.6	35.0	40.8
20	43.8	44.6	43.3	44.1	44.3	44.5	44.2	43.0
21	30.9	32.0	31.0	31.0	31.6	31.0	31.4	30.3
22	37.2	38.6	37.8	38.5	38.6	34.6	38.5	37.5
23	28.6	29.2	26.4	28.6	28.5	28.6	28.9	28.1
24	15.6	17.2	21.4	16.3	16.4	16.4	16.3	15.6
25	16.4	17.1	15.7	16.9	16.6	17.3	14.8	17.1
26	18.7	13.9	18.5	19.7	12.9	19.0	19.3	18.5
27	23.4	19.4	23.3	18.7	23.9	14.2	65.9	23.0
28	28.1	29.9	28.5	29.6	29.0	17.5	28.7	28.1
29	28.5	29.3	28.6	28.5	28.4	28.8	30.8	27.8
30	181.8	179.7	181.8	178.0	178.0	178.3	178.2	177.7

[a] Spectra run at 150 MHz, δ in ppm.
[b] Measured in $CDCl_3$ relative to TMS.
[c] Measured in pyridine-d_5 relative to TMS at 125 MHz.
[d] Measured in DMSO-d_6 relative to TMS.
[e] Measured in acetone-d_6 relative to TMS.

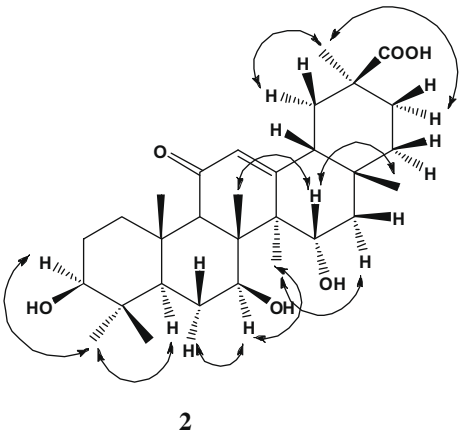

2

Fig. 3. Important NOE correlations of **2**.

stereochemistry at C-18 of metabolite **6** could have proceeded, enzymatically, in the same way described by Ignatov et al., 2003, or may be *via* the formation of a new double bond between C-18 and C-19 followed by reduction.

NMR data of metabolite **7** (Tables 1 and 2) indicated a dihydroxylated derivative of glycyrrhetinic acid. Four oxygenated carbon resonances, other than the carbonyl and the carboxylic groups, were detected in the ^{13}C NMR spectrum of **7** (Table 2) at δ 65.9, 69.0, 78.2 and 87.7. These were discriminated by DEPT experiment into one methylene, two methines and one quaternary carbon atom. The methine carbon resonance at δ 78.2 which was correlated by HMQC to the proton signal at δ 3.15 (*dd*, J = 4.4, 11.7 Hz) was assigned to position 3. The other methine carbon resonating at δ 69.0 was correlated to another *dd* at δ 3.84 (J = 5.8, 11.4 Hz) in the ^{1}H NMR spectrum (Table 1) and could be assigned to

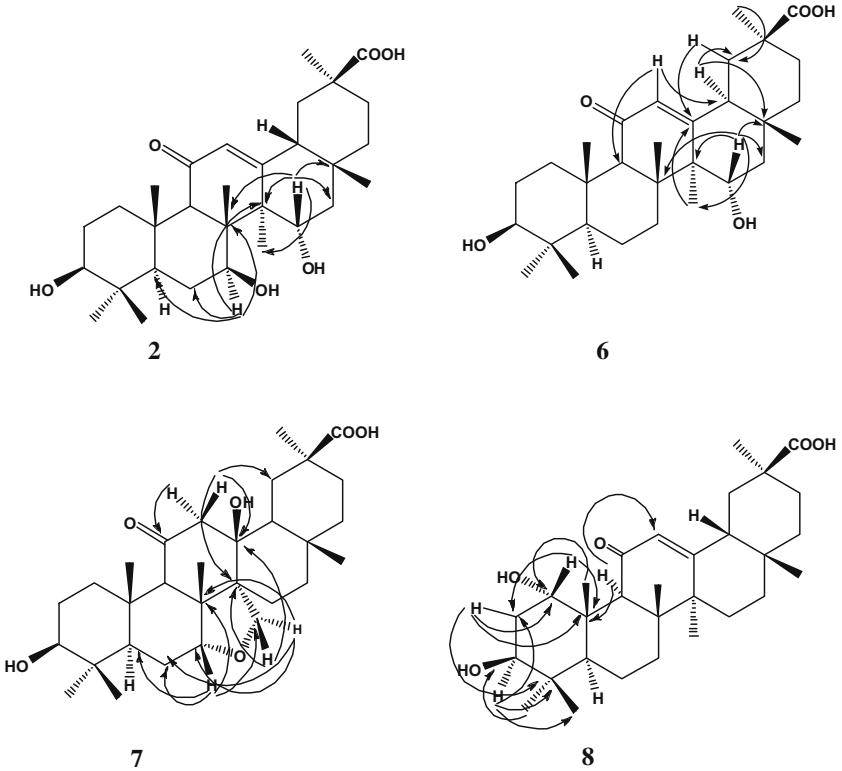

2 6 7 8

Fig. 2. Important HMBC correlations of **2**, **6**, **7** and **8**.

position 7 by HMBC (Fig. 2). The methylene carbon at δ 65.9 was correlated to two proton signals at δ 4.27 (*dd*, *J* = 8.6, 2.2) and 3.71 (*d*, *J* = 8.6). The coupling constant between those protons (8.6 Hz) is reasonable for two gem protons adjacent to an atom bearing a lone pair (Williams and Fleming, 1997). These protons showed cross peaks in the HMBC spectrum with carbon atoms at positions 7, 8, 13 and 14 (Fig. 2) suggesting oxygenation at C-27 and cyclization between C-27 and C-7. This was confirmed by detecting signals due to only six methyl groups in both ^{1}H- and DEPT spectra of **7**. An ether bridge between C-27 and C-7 was suggested based on the observation of a molecular ion peak in HRESIMS (negative ion mode) at *m/z* 502.3239 corresponding to the molecular formula $C_{30}H_{46}O_6$ (calc. 502.3294) and cross peaks in the HMBC spectrum (Fig. 2) between H-7 (δ 3.84, *dd*, *J* = 5.8, 11.4 Hz) and C-27 (δ 65.9), between H-27 (δ 3.71, *d*, *J* = 8.6 Hz) and each of C-6 (δ 31.8) and C-7 (δ 69.0). Based on the large coupling constant of H-7 (11.4 Hz) as well as the observation of an upfield shift of H-7 by 0.14 ppm, compared to the same proton in metabolite **5**, this proton was concluded to have a β axial configuration. This was supported by Dreiding model, where the shielding of C-26 in metabolite **5** by 6.4 ppm, compared to the same carbon in **7**, was attributable to γ-gauche interaction between this carbon and the β-oriented OH group at position 7. Such an effect vanished in **7** and can be explained only when the oxygen function at C-7 is α-oriented. The disappearance of the carbon resonances due to the olefinic carbons at positions 12 and 13 (δ 128.5 and 169.5, respectively in glycyrrhetinic acid) together with the appearance of two new methylene proton signals in ^{1}H NMR spectrum at δ 2.09 and 2.96 (*d*, *J* = 15.7 Hz) which were correlated to a methylene carbon resonance at δ 54.3 as well as the downfield shift of C-11 by 8.0 ppm (δ 200.5–208.5), placed the remaining oxygen function at C-13. This was confirmed through HMBC, where cross peaks were observed between C-13 (δ 87.7) and each of H-12 and H-27. Moreover; the large coupling constant of H-12 (15.7 Hz) is consistent with that expected for geminal protons situated between a π-bond and an atom with a lone pair (Williams and Fleming, 1997). Comparing the chemical shifts of C-13 and carbon atoms in its vicinity to published data of some triterpenes hydroxylated at this position (Mahato and Kundu, 1994), the hydroxyl group was assigned to be β-oriented. Thus the structure of metabolite **7** was confirmed to be 13β-hydroxy-7α, 27-oxy-12-dihydro-18β-glycyrrhetinic acid which is a new natural product.

The monohydroxy derivatives at positions 7 and 27 *viz*. 7α-hydroxy and 27-hydroxy were not isolated in this study, nor were the free uncyclized hydroxyl form of **7**. These metabolites could be present as minors; otherwise metabolite **7** is rapidly formed following hydroxylation of glycyrrhetinic acid at the corresponding positions.

Metabolite **8** was tentatively identified as the new natural product 1α-hydroxy-18β-glycyrrhetinic acid. ESIMS (positive ion mode) gave a molecular ion peak at *m/z* 486 $[M]^+$, corresponding to the molecular formula $C_{30}H_{46}O_5$. Monohydroxylation was suggested based on the detection of a new methine proton multiplet in the ^{1}H NMR spectrum (Table 1) at δ 4.38. This proton together with the other methine signal at δ 3.44 (*ddd*, 4.9, 5.7, 11.5 Hz, H-3) were correlated by HMQC to one carbon resonance at δ 70.6. This resonance was interpreted as two coincident methine carbons from peak intensity (DEPT spectrum) and was assigned to positions 1 and 3, respectively by HMBC experiment. HMBC spectrum (Fig. 2) showed cross peaks between H-1 (δ 4.38, *m*) and each of C-2 and C-10 (δ 33.9, 40.8), between C-1 (δ 70.6) and each of C-25 methyl protons (δ 1.00, s), H-2 (δ 1.76, m) and H-9 (δ 3.25, s). Assignment at position 3 was similarly deduced by observing cross peaks between H-3 (δ 3.44, *ddd*, 4.9, 5.7, 11.5 Hz) and each of C-2, C-4, C-23 and C-24 (δ 33.9, 38.7, 28.4 and 15.6). This assignment was confirmed by the deshielding of C-2 by 6.7 ppm due to the mutual β-effect of hydroxylation at carbons 1 and 3 respectively and also the deshielding of C-10 by 3.7 ppm due to β-effect of the hydroxylated C-1. The hydroxyl group at C-1 was deduced to be axial (α-oriented), based on the observation of shielding of C-5 and C-9 by 8.6 and 9.3 ppm, respectively due to typical γ-gauche interaction between these carbons and the axial hydroxyl at C-1. Further evidence for orientation at C-1 was derived also by observing shielding of C-3 by 8.3 ppm compared to glycyrrhetinic acid (Table 2), again due to γ-gauche interaction with the axial hydroxyl at C-1 (Mahato and Kundu, 1994).

Several mechanisms have been suggested to contribute to the hepatoprotective and the antiviral activities of glycyrrhetinic acid. Those involved in hepatoprotection, included antioxidant activity by direct free radical scavenging activity (Kiso et al., 1984) as well as inhibition of free radical generation and inhibition of cytochrome p450 2E1 expression (Jeong et al., 2002). The antiviral activity was attributed to an immuno-modulating activity through stimulation of nitric oxide (NO) production (Jeong and Kim, 2002). NO is a host defence molecule produced by the enzyme NO synthase in a variety of immune cells. It has been identified to inhibit the growth of microorganisms including bacteria, fungi and viruses (Taylor et al., 1998). Hence, glycyrrhetinic acid metabolites **2** and **7** were tested for their hepatoprotective activities using assays for measuring protection against lipid peroxidation both *in vivo* and *in vitro*. Lipid peroxidation can proceed in a non-enzymatic way *in vitro*. The mechanism of iron-ascorbate-accelerated lipid peroxidation is discussed by Fukuzawa et al. (1993), Bondet et al. (2000) and Zadlo et al. (2006). Also, the effect on nitric oxide production in rat macrophages was tested.

Subcutaneous injection of albino mice with glycyrrhetinic acid metabolites **2** and **7** at doses of 50 mg kg^{-1}, significantly decreased the level of liver transaminases (ALT and AST) which are markers for liver injury. An effect that was not statistically different from that of glycyrrhetinic acid (Table 3). Both metabolites were also effective in lowering the liver oxidative stress status induced by CCl_4-intoxication and expressed as the concentration of malondialdehyde (MDA). MDA is a major product of lipid peroxidation which is used as a marker of oxidative liver damage. Again the effect of both metabolites was not significantly different from that of glycyrrhetinic acid ($p > 0.05$), although metabolite **2** performed far better than both glycyrrhetinic acid and metabolite **7** in the *in vitro* assay that measures the protective effect of the test metabolites against iron-ascorbate stimulated lipid peroxidation (61 ± 6.1 *versus* 12 ± 4.5 and 20 ± 3.7, respectively) and measured as percentage protection against a fully peroxidized control (Tables 3 and 4(. Glycyrrhetinic acid was shown before to stimulate nitric

Table 3
Effects of pretreatment with glycyrrhetinic acid and metabolites **2** and **7** on carbon tetrachloride-induced hepatotoxicity in mice.

	Normal	CCl_4	Glycyrrhetinic acid	Metabolite 2	Metabolite 7
ALT (U/L)	156 ± 26.0	5568 ± 219.9	564 ± 268.4[a]	1516 ± 172.8[a]	1748 ± 230.7[a]
AST (U/L)	246 ± 16.0	3760 ± 89.8	520 ± 168.2[a]	1194 ± 259.5[a]	1096 ± 74.6[a]
MDA (nmol/g liver)	255 ± 27.4	473 ± 62.5	204 ± 39.8[a]	161.3 ± 16.9[a]	173 ± 19.5[a]

Data expressed as means ± SEM.
[a] Significant from CCl_4 at $p < 0.001$.

Table 4
Protective effect of glycyrrhetinic acid and metabolites **2** and **7** on iron-ascorbate-induced lipid peroxidation.[a]

Treatment (1 mg ml^{-1})	Antioxidant index (AI)[a]
Glycyrrhetinic acid	12 ± 4.5
Metabolite **2**	61 ± 6.1
Metabolite **7**	20 ± 3.7

[a] Data are expressed as percentage protection compared to a fully peroxidized control ± SEM.

Table 5
Effect of glycyrrhetinic acid and metabolites **2** and **7** on NO production in CCl_4 treated rat macrophages.

	NO (μM)[a]			
	1.5 μM	12.5 μM	25.0 μM	50.0 μM
Glycyrrhetinic acid	11.8 ± 1.7	35.9 ± 1.9	37.9 ± 1.2	60 ± 0.6
Metabolite **2**	13.0 ± 2.0	27.6 ± 2.4	28.1 ± 1.0	56.7 ± 0.4
Metabolite **7**	21.7 ± 2.9	36.9 ± 1.6	44.2 ± 1.0	71.6 ± 0.3

[a] NO concentration for non treated cells 8.29 μM and for CCl_4 treated cells 12.8 μM. Data are expressed as means ± SEM.

oxide (NO) production in resting macrophages as well as those stimulated with lipopolysaccharide (Jeong and Kim, 2002). We evaluated glycyrrhetinic acid and its metabolites **2** and **7** for their effect on the production of NO in rat macrophages treated with CCl_4. NO level in resting cells incubated for 24 h was as low as 8.29 μM. Treatment with CCl_4 (10 μM) only increased its level to 12.8 μM. Glycyrrhetinic acid and its metabolites significantly stimulated NO production in a dose dependant manner up to concentrations of 50 μM (Table 5). From the data presented in Tables 3–5 and the above discussion, it could be concluded that both of the tested compounds are active glycyrrhetinic acid metabolites that could be useful as hepatoprotective drugs. Both performed better than the substrate in all assays. The use of these metabolites as applied therapeutics still needs more experimental evidence. The other metabolites could be active as well, but their testing needs further scaling up and isolation of larger quantities as they are minor products.

3. Experimental

3.1. General experimental procedures

Optical rotations were obtained on JASCO P-1020 Polarimeter (Tokyo, Japan). ^{1}H, ^{13}C NMR, DEPT, ^{1}H-^{1}H COSY, HMBC and HMQC spectra were obtained with Bruker dpx 500 and Bruker AMX-600 high-field spectrometers (Bruker Instruments, UK and USA), operating at 500 and 600 MHz (^{1}H) and 125 and 150 MHz (^{13}C). Mass spectrometry obtained as electrospray ionization spectra (ESIMS) was taken on a VG-ZAB-HF reversed-geometry (BE configuration, where B is a magnet sector and E is an electrostatic analyzer) mass spectrometer (MS) VG Analytical Inc. (USA). Column chromatography was performed on silica gel (70-230 mesh, Merck, Germany). TLC was carried out on precoated Si gel 60 GF_{254} (Merck, USA) plates. Developed chromatograms were visualized by spraying developed plates with 0.01% vanillin/H_2SO_4, followed by heating until maximum development of the spots colour. Preparative scale TLC was carried out on 1 mm-thick Si gel plates. Solvents were reagent grade. Thiobarbituric acid (Sigma, UK). 1,1,3,3-Tetraethoxypropane used as a standard for calibration of malondialdehyde (MDA), kits for analysis of liver enzymes, sulphanilamide and N-(1-naphthyl-ethylenediamine) (Biodiagnostics, Egypt).

3.2. Substrate

Glycyrrhetinic acid (**1**) used in this study was purchased from Sigma (USA) and its identity was confirmed by comparison of its different spectroscopic data to those published in the literature (Komoda, 1984).

3.3. Fermentation method

Fermentation in liquid cultures was carried out according to the standard two-stage fermentation protocol (Betts et al., 1974). For screening experiments, solid cultures kept on either potato dextrose agar (PDA) or sabaraud maltose agar (SMA) of the following organisms were used: *A. pseudocylinderospora* ATCC 24169, *Amycolata autotrophica* ATCC 35203, *Aspergillus alliaceus* UI 315, *A. niger* ATCC 9142, *Aspergillus ochraceous* ATCC 1008, *Bacillus cereus* NRRL 14591b, *Bacillus megaterium* ATCC 14581, *Beauveria bassiana* ATCC 7159, *Botrytis alli* NRRL 2502, *Candida tropicalis* UI 2312, *Comamonas testosteroni* ATCC 11996, *C. echinulata* ATCC 8688a, *Cunninghamella elegans* ATCC 9245, *Curvularia lunata* NRRL 2178, *G. viride* ATCC 10097, *Mortierella isabellina* ATCC 38063, *Mucor mucedo* UI 5513, *Nocardia species* NRRL 5646, *Rhizopus stolonifer* NRRL 1478, *Rhodtorula rubra* ATCC 20129, *Sepedonium chrysanthosporum* ATCC 13378, *Streptomyces griseus* ATCC 13273 and *Thamnidium elegans* ATCC 18191. Each culture was used separately to inoculate 100 ml flasks containing one fifth of their volume of the following medium: 2% glucose, 0.5% soybean meal, 0.5% yeast extract, 0.5% NaCl, 0.5% K_2HPO_4. The pH was adjusted to 7.0 before autoclaving for 20 min at 121 °C and 15 psi. The inoculated flasks were incubated at 27 °C and 250 rpm for 72 h (stage I cultures) before being used to inoculate stage II culture flasks, in which 10% inoculum volumes of stage I were used to inoculate another sterile medium and were incubated under the same conditions for 24 h. Glycyrrhetinic acid (30 mg) dissolved in 1.5 ml of CH_2Cl_2–DMSO (1:1) was added to the 24 h-old stage II cultures in 50 μl aliquots to give a final concentration of 1 mg substrate per flask. The flasks were incubated again and sampled periodically for analysis.

3.4. Sampling

Samples of 1 ml were taken after 12, 24, 36 and 48 h and then every other day for 2 weeks following substrate addition. Each sample was extracted by shaking with 0.5 ml of EtOAc and spun at 3000 g for 1 min in a desktop centrifuge. The extracts were concentrated and spotted on Si gel GF_{254} TLC plates, developed with CH_2Cl_2–MeOH (94:6). The developed chromatograms were visualized by spraying with vanillin/H_2SO_4, followed by heating with a heating gun until maximum development of the spots colour.

3.5. Preparative scale conversion

Glycyrrhetinic acid was added to stage II cultures of microorganisms which gave the best results in screening. *A. pseudocylinderospora* ATCC 24169 and *C. echinulata* ATCC 8688a cultures received 1 g each of glycyrrhetinic acid while *G. viride* ATCC 10097 received 100 mg. The substrate was added at concentration of 1 mg per ml of culture medium prepared as above in 1 l flasks. After incubation for 2 weeks under the same conditions, the broth and the fungal mycelia were combined, homogenized in a blender and exhaustively extracted with EtOAc 3 × 1 l. The extract was dried over anhydrous Na_2SO_4 and concentrated under reduced pressure to yield a 900, 1250 and 270 mg of residue, respectively.

3.6. Isolation and purification of the metabolites

The EtOAc extract from scaling up the reaction with *A. pseudocylinderospora* ATCC 24169 (875 mg) was chromatographed on a silica gel column (70 × 1 cm) eluted with mixtures of CH_2Cl_2 and MeOH. Fractions eluted with 3% MeOH in CH_2Cl_2 (226 mg) contained one major spot (R_f 0.55, CH_2Cl_2–MeOH, 96:4) and several minors which are more polar. Rechromatography on silica gel column using the same solvent system afforded metabolite **2** (160 mg). Fractions eluted with CH_2Cl_2 containing 6–10% MeOH (155 mg) were shown to contain a mixture of three spots on RP-18 silica gel plates, using 50% MeOH in water as solvent system. This mixture was not further purified.

Fractionation of the EtOAc extract from scaling up the reaction with *G. viride* ATCC 10097 (270 mg) on a silica gel column (50 × 1 cm) and elution with 3% MeOH in hexane–CH_2Cl_2 (1:2) yielded one major fraction containing one major spot (65 mg). It was further purified on preparative TLC using 5% MeOH in hexane–CH_2Cl_2 (1:1) to give pure metabolite **3** as colourless prisms (42 mg, R_f 0.27, 5% MeOH in hexane–CH_2Cl_2, 2:1). The EtOAc extract from scaling up the reaction with *C. echinulata* ATCC 8688a (1.2 g) was chromatographed on a column of silica gel (70 × 1.5 cm) and eluted with mixtures of hexane and CH_2Cl_2 (1:2) containing MeOH (2.5–10%). Fifty millilitre fractions were collected and similar fractions pooled and monitored by TLC, using vanillin/H_2SO_4 as spray reagent to afford three major groups (A–C). Group A (fractions 28–30, 475 mg) was further subjected to CC on silica gel (50 × 1.5 cm), isocratically eluted with 5% isopropyl alcohol in hexane containing 0.25% HCOOH. Ten millilitre fractions were collected to afford metabolite **4** [32 mg, R_f 0.63, hexane–CH_2Cl_2 (1:1) containing 12% isopropyl alcohol], metabolite **5** [22 mg, R_f 0.58, hexane–CH_2Cl_2 (1:1) containing 12% isopropyl alcohol] and a mixture (301 mg). Group B (fractions 33–42, 88 mg) was similarly treated as above to afford 6 and 54 mg of metabolites **6** [R_f, 0.56, hexane–CH_2Cl_2 (1:1) containing 12% isopropyl alcohol] and **7** [R_f, 0.50, hexane–CH_2Cl_2 (1:1) containing 12% isopropyl alcohol]. Group C (fraction 66, 35 mg) was purified on a silica gel column (50 × 1 cm) and eluted with hexane–CH_2Cl_2 (1:1) containing 10% MeOH to afford a mixture of three spots (R_f, 0.61, 0.55, 0.50, hexane–CH_2Cl_2–MeOH, 4:4:2, 26 mg). It was separated on preparative TLC using 15% MeOH in hexane–CH_2Cl_2 (1:1), three developments, to afford 1 mg of pure metabolite **8** [R_f 0.61, hexane–CH_2Cl_2–MeOH, 4:4:2].

3.7. 7β,15α-Dihydroxy-18β-glycyrrhetinic acid (*2*)

Colourless cubic crystals, m.p 244 °C, 160 mg, R_f 0.55 (CH_2Cl_2–MeOH, 96:4), $[\alpha_D^{24}]$ + 1.813 (MeOH; c 1.0). ^1H and ^{13}C NMR (500, 125 MHz, pyridine-d_5) (Tables 1 and 2), HRESIMS (negative ion mode) *m/z* (rel. int.) 502.3251 (33) $[M]^-$ (calc. 502.3294 for $C_{30}H_{46}O_6$), 501.3229 (100) $[M-1]^-$, 487.2760 (5) $[M-CH_3]^-$, 485.2802 (26) $[M-OH]^-$.

3.8. 3-Oxo-18β-glycyrrhetinic acid (*3*)

Colourless prisms, m.p 283–285 °C (dec.), 42 mg, R_f 0.27, 5% MeOH in hexane–CH_2Cl_2, 2:1, $[\alpha_D^{24}]$ + 0.334 (MeOH; c 0.2). ^1H and ^{13}C NMR (600, 150 MHz, $CDCl_3$) (Tables 1 and 2), HRESIMS (negative ion mode) *m/z* (rel. int.) 468.3210 (42) $[M]^-$ (calc. 468.3239 for $C_{30}H_{44}O_6$). ESIMS (negative mode) *m/z* (rel. int.) 468 (35) $[M]^-$, 467 (100) $[M-1]^-$, 453 (15) $[M-CH_3]^-$, 451 (5) $[M-OH]^-$, 440 (6) $[M-CO]^-$and cluster ions at *m/z* 935 (2) $[2M-1]^-$, 958 (2.5) $[2M-1+Na]^-$.

3.9. 15-Hydroxy-18β-glycyrrhetinic (*4*)

Amorphous solid, 32 mg, R_f 0.63, hexane–CH_2Cl_2 (1:1) containing 12% isopropyl alcohol, $[\alpha_D^{24}]$ + 0.348 (MeOH; c 1.0). ^1H and ^{13}C NMR (600, 150 MHz, acetone-d_6) (Tables 1 and 2), ESIMS (negative ion mode) *m/z* (rel. int.) 486 (34) $[M]^-$, 485 (100) $[M-1]^-$ and cluster ions at *m/z* 972 (2) $[2M]^-$, 995 (1) $[2M+Na]^-$.

3.10. 7β-Hydroxy-18β-glycyrrhetinic acid (*5*)

Amorphous solid, 22 mg, R_f 0.58, hexane–CH_2Cl_2 (1:1) containing 12% isopropyl alcohol, $[\alpha_D^{24}]$ + 0.370 (MeOH; c 1.0). ^1H and ^{13}C NMR (600, 150 MHz, acetone-d_6) (Tables 1 and 2), ESIMS (negative ion mode) *m/z* (rel. int.) 486 (35) $[M]^-$, 485 (100) $[M-1]^-$, 441 (13) $[M-COOH]^-$.

3.11. 15α-Hydroxy-18-glycyrrhetinic acid (*6*)

Amorphous solid, 6 mg, R_f 0.56, hexane–CH_2Cl_2 (1:1) containing 12% isopropyl alcohol, $[\alpha_D^{24}]$ + 0.402 (MeOH; c 1.0). ^1H and ^{13}C NMR (600, 150 MHz, acetone-d_6) (Tables 1 and 2), ESIMS (negative ion mode) *m/z* (rel. int.) 486 (32) $[M]^-$, 485 (100) $[M-1]^-$, 441 (3) $[M-COOH]^-$, 390 (7), 255 (6), 121 (8).

3.12. 13β-Hydroxy-7 α, 27-oxy-12-dihydro-18β-glycyrrhetinic acid (*7*)

Needle crystals, m.p 296° C, 54 mg, R_f 0.50, hexane–CH_2Cl_2 (1:1) containing 12% isopropyl alcohol, $[\alpha_D^{24}]$ + 0.249 (MeOH; c 0.5). ^1H and ^{13}C NMR (600, 150 MHz, acetone-d_6) (Tables 1 and 2), HRESIMS (negative ion mode) *m/z* 502.3231 $[M]^-$ (calc. 502.3294 for $C_{30}H_{46}O_6$). ESIMS (negative ion mode) *m/z* (rel. int.) 502 (32) $[M]^-$, 501 (100) $[M-1]^-$, 487 (11) $[M-CH_3]^-$, 485 (30) $[M-OH]^-$, 453 (9) [485-1-CH_2OH].

3.13. 1-Hydroxy-18β-glycyrrhetinic acid (*8*)

Amorphous solid, 1 mg, R_f 0.61, hexane–CH_2Cl_2–MeOH, 4:4:2, $[\alpha_D^{24}]$ + 0.241 (MeOH; c 0.1). ^1H and ^{13}C NMR (600, 150 MHz, DMSO-d_6) (Tables 1 and 2), ESIMS (positive ion mode) *m/z* (rel. int.) 487 (51) $[M+1]^+$, 486 (7) $[M]^+$, 469 (32) $[M-OH]^+$, 275 (25), 191 (64), 509 (1) $[M+Na]^+$, 972 (1) $[2M]^+$, 974 (100) $[2M+2]^+$, 996 (13) $[2M+1+Na]^+$.

3.14. Iron-ascorbate stimulated lipid peroxidation in liver homogenate

The assay was carried out in liver homogenate according to a method described by Jeong et al. (2002) with slight modifications. Briefly, a 10% mice liver homogenate in 1.1% w/v KCl was used. The reaction mixture consisted of 250 µl liver homogenate, 50 µl of 0.1 mM ascorbic acid, 50 µl of 4 mM $FeCl_3$, 750 µl thiobarbituric acid (0.8% w/v) in sodium dodecyl sulfate (1.1% w/v), 750 µl acetic acid (20% v/v) and 50 µl of different concentrations of the test substances suspended in sodium dodecyl sulfate (8.1% w/v). The reaction mixture was heated at 95 °C and the formed malondialdehyde, was quantified following a modified thiobarbituric acid reactive species assay as described by Baratta et al. (1998). 1,1,3,3-Tetraethoxypropane was used as a standard for calibration of MDA.

3.15. In vivo hepatoprotective assay

Female albino mice (20–25 g) were allowed free access to a standard meal and tap water and maintained in a controlled environment at 25 ± 2 °C under a 12 h dark/light cycle and acclimatized at least for one week before starting the experiment. Animals were divided into groups of six, each. The treated groups received the

test compounds for four consecutive days (50 mg kg^{-1}, subcutaneously, suspended in corn oil). Normal group received corn oil). The control group was treated with CCl_4 (2 ml kg^{-1}, i.p., dissolved in corn oil as single dose before the last dose of the test compounds). Twenty-four hours after the last treatment, animals were anesthetized by diethyl ether and blood was collected by puncture of the retro-orbital plexus to determine the ALT and AST activities. Animals were then killed by cervical dislocation. Livers were dissected and quickly frozen and kept for liver peroxidation analysis.

3.16. Hepatotoxicity evaluation

Serum ALT and AST activities were measured using a spectrophotometric diagnostic kit according to the manufacturer instructions. Liver peroxidation was measured by the formation of the thiobarbituric acid reactive material malondialdehyde in 10% liver homogenate, following a modified thiobarbituric acid reactive species assay (Baratta et al., 1998).

3.17. Nitric oxide production in peritoneal rat macrophages

The assay was carried out according to methods described by Ma and Kovanen (1995) and Yang et al. (2004). Peritoneal rat macrophages (PMCs) were isolated by slow injection of 25 ml of 0.25% trypsin-0.02% EDTA–Na_2 into the rat abdominal cavity. The fluid was removed from the peritoneal cavity under sterile conditions after 15 min. Cellular components were isolated using low speed (1500 rpm) centrifugation for 10 min at 4 °C. Pellets were then washed briefly with phosphate buffered saline (PBS) and resuspended in RPMI-1640 medium supplemented with 10% (v/v) foetal calf serum (FCS), penicillin (100 U/ml) and streptomycin (0.1 mg/ml). Cells were placed into 25 cm^2 tissue-culture flasks and incubated overnight at 37 °C in a humidified 5% CO_2 atmosphere. PMCs were passaged by dissociating the confluent monolayer with 0.25% trypsin-0.02% EDTA–Na_2 and were reseeded in 96-well plates (3×10^5 cells/well) and incubated in the same medium for 24 h. Non-adherent material was removed the next day with two brief washes using PBS. The adherent population was then incubated at 37 °C, 5% CO_2 in fresh culture medium for 2 h. The test compounds dissolved in dimethyl formamide (DMF) were then added at concentrations ranging from 1.5 to 50 μM. The concentration of DMF did not exceed 0.1% v/v. CCl_4 (10 μM) was then added and the plates incubated for 24 h. Nitric oxide was assayed in the supernatants using Griess reagent. The assay depends on diazotization of sulphanilamide with the produced nitrite in acid medium and then formation of azo dye by coupling with N-(1-naphthyl-ethylenediamine dihydrochloride, NEDA). The formed complex has a bright reddish purple colour, which can be measured at 540 nm. Concentrations were determined by comparing absorbance of test solutions to that of a standard sodium nitrite solution (50 μM). Briefly, the reaction was carried out by mixing 100 μl of the culture supernatants with 1 ml of 10 mM sulphanilamide containing 1% orthophosphoric acid and standing for 5 min, followed by adding 100 μl of 1 mM NEDA, standing for another 5 min. The absorbance of the developed colour was measured at 540 nm. Appropriate blanks were carried out for both sample and standard. Concentration of NO was calculated using the following formula: $\mu M = A_{sample}/A_{standard} \times 50$.

3.18. Statistical analysis

Differences among all groups were analyzed by one-way analysis of variance (ANOVA) followed by Tukey–Kramer multiple comparisons test. $N = 6$.

Acknowledgements

This work is a part of the research project "applications of biotechnology in drug production, development and metabolic studies", funded by Mansoura University Research Treasury Unit. The authors gratefully acknowledge assistance from Prof. F.A. Badria and Mr. A. Abbas, Department of Pharmacognosy, Faculty of Pharmacy, Mansoura University, in carrying out the biological assays.

References

Arase, Y., Ikeda, K., Murashima, V., Chayama, K., Tsubota, A., Koida, I., Suzuki, Y., Saitoh, S., Kobayashi, M., Kumoda, H., 1997. The long term efficacy of glycyrrhizin in chronic hepatitis C patients. Cancer 79, 1494–1500.

Baratta, M., Dorman, H., Deans, S., Figueiredo, A.C., Barroso, J., Ruberto, G., 1998. Antimicrobial and antioxidant properties of some commercial essential oils. Flav. Fragr. J. 13, 235–244.

Barran, J., Langford, D., Pitzele, B., 1974. Synthesis and biological activities of substituted glycyrrhetic acids. J. Med. Chem. 17, 184–191.

Betts, R., Walters, D., Rosazza, J., 1974. Microbial transformation of antitumor compounds. I. Conversion of acronycine to 9-hydroxyacronycine by *Cunninghamella echinulata*. J. Med. Chem. 17, 599–602.

Bondet, V., Cuvelier, M., Berset, C., 2000. Behaviour of phenolic antioxidants in a partitioned medium: focus on linoleic acid peroxidation induced by iron/ascorbic acid system. J. Am. Oil Chem. Soc. (JAOCS) 77, 813–819.

Canonica, L., Ferrari, M., Jommi, G., Pagnoni, U., Pelizzoni, F., Ranzi, B., Maroni, S., Nencini, T., Salvatori, T., 1967. Ossidazioni microbiologiche di triterpenoidi. Nota II. Acidi 15α-idrossi-glicerretico e 7β, 15α-diidrossi-glicerretico. Gazz. Chim. Ital. 97, 1032–1051.

Chung, W., Lee, S.H., Kim, J., Sung, N., Hwang, B., Lee, S.Y., Yu, C., Lee, H., 2001. Effect of the extracts from *Glycyrrhiza uralensis* Fisch. on the growth characteristics of human cell lines: antitumor and immune activation activities. Cytotechnology 37, 55–64.

Fukuzawa, K., Seko, T., Minami, K., Terao, J., 1993. Dynamics of iron-ascorbate-induced lipid peroxidation in charged and uncharged phospholipid vesicles. Lipids 28, 497–503.

Ignatov, D., Prokof'ev, Yu., Ipatova, O., Timofeev, V., Medvedeva, N., Misharin, Yu., 2003. A simple method for preparation of 18β-glycyrrhetinic acid and its derivatives. Russ. J. Bioorg. Chem. 29, 390–394.

Jeong, H., Kim, J., 2002. Induction of inducible nitric oxide synthase expression by 18β-glycyrrhetinic acid in macrophages. FEBS Lett. 513, 208–212.

Jeong, H., You, H., Park, S., Moon, A., Chung, Y., Kang, S., Chun, H., 2002. Hepatoprotective effects of 18β-glycyrrhetinic acid on carbon tetrachloride-induced liver injury: inhibition of cytochrome p450 2E1 expression. Pharmacol. Res. 46, 221–227.

Kieslich, K., 1976. Microbial Transformations of Non-steroid Cyclic Compounds. John Wiley and Sons, New York.

Kiso, Y., Tohkin, M., Hikino, H., Hattori, M., Sakamoto, T., Namba, T., 1984. Mechanism of antihepatotoxic activity of glycyrrhizin. I. Effect of free radical generation and lipid peroxidation. Planta Med. 50, 298–302.

Komoda, Y., 1984. Nuclear magnetic resonance of 18β-glycyrrhetinic acid and its related compounds. Rep. Inst. Med. Dent. Engin. 18, 39–44 (in Japanese).

Luo, H., Huang, W., Zhang, Z., Wu, Q., Huang, M., Zhang, D., Yang, F., 2004. 18β-glycyrrhetinic acid-induced apoptosis and relation with intracellular Ca^{2+} release in human breast carcinoma cells. Chi. Ger. J. Clin. Oncol. 3, 137–140.

Ma, H., Kovanen, P., 1995. Ig E-dependent generation of foam cells: an immune mechanism involving degranulation of sensitized mast cells with resultant uptake of LDL by macrophages. Arterioscl. Thromb. Vasc. Biol. 15, 811–819.

Mahato, S., Kundu, A., 1994. ^{13}C NMR spectra of pentacyclic triterpenoids – a compilation and some salient features. Phytochemistry 37, 1517–1575.

Mahato, S., Nandy, A., Roy, G., 1992. Triterpenoids. Phytochemistry 31, 2199–2249.

Nabekura, T., Yamaki, T., Ueno, K., Kitagawa, S., 2008. Inhibition of p-glycoprotein and multidrug resistance protein 1 by dietary phytochemicals. Cancer Chemother. Pharmacol. 62, 867–873.

Ryu, S., Choi, S., Lee, S., Lee, C., No, Z., Ahn, J., 1994. Antitumor triterpenes from medicinal plants. Arch. Pharmacol. Res. 17, 375–377.

SimeÓ, Y., Kroutil, W., Faber, K., 2007. Biocatalytic deracemization: dynamic resolution, stereoinversion, enantioconvergent processes and cyclic deracemization. In: Patel, R. (Ed.), Biocatalysis in the Pharmaceutical and Biotechnology Industries. CRC Press, London, pp. 27–51 (Chapter 2).

Taylor, B., Alarcon, L., Billiar, T., 1998. Inducible nitric oxide synthase in liver: regulation and function. Biokhimiya 63, 766–781.

Van Rossum, T., Vulto, A., De Man, R., Brouwer, J., Schlam, S., 1998. Review article: glycyrrhizin as potential treatment for chronic hepatitis C. Ail. Pharmacol. Ther. 12, 199–205.

Williams, D., Fleming, I., 1997. Spectroscopic Methods in Organic Chemistry, fifth ed. McGraw-Hill, Maidenhead, UK, pp. 98–99.

Xin, X., Liu, Y., Yo, M., Guo, H., Guo, D., 2006. Microbial transformation of glycyrrhetinic acid by *Mucor polymorphosporus*. Planta Med. 72, 156–161.

Yamada, Y., Nakamura, A., Yamamoto, K., Kikuzaki, H., 1994. Transformation of glycyrrhezic acid by *Aspergillus* spp. Biosci. Biotechnol. Biochem. 58, 436–437.

Yang, X., Ye, R., Kong, Q., Yang, Q., Dong, X., Yu, X., 2004. CD40 is expressed on rat peritoneal mesothelial cells and upregulates ICAM-1 production. Nephrol. Dial. Transplant. 19, 1378–1384.

Yoshida, K., Furihata, K., Habe, H., Yamane, H., Omori, T., 2001a. Isolation of transposon Tn5 mutant affected in the metabolism of 18β-glycyrrhetinic acid. Biotechnol. Lett. 23, 873–879.

Yoshida, K., Furihata, K., Habe, H., Yamane, H., Omori, T., 2001b. Microbial transformation of 18β-glycyrrhetinic acid by *Sphingomonas paucimobilis* strain G5. Biotechnol. Lett. 23, 1619–1624.

Yoshida, K., Furihata, K., Yamane, H., Omori, T., 2001c. Metabolism of 18β-glycyrrhetinic acid in *Sphingomonas paucimobilis* strain G5. Biotechnol. Lett. 23, 253–258.

Zadlo, A., Rozanowska, M., Burke, J., Sarna, T., 2006. Photobleaching of retinal pigment epithelium melanosomes reduces their ability to inhibit iron-induced peroxidation of lipids. Pig. Cell Res. 20, 52–60.